Motion Compensated Fan-Beam CT by Enforcing Fourier Properties of the Sinogram

06/25/2014

Martin Berger[1], Andreas Maier[1], Yan Xia[1], Joachim Hornegger[1] and Rebecca Fahrig[2]

1) Pattern Recognition Lab, Friedrich-Alexander-University Erlangen-Nuremberg, Germany
2) Department of Radiology, Stanford University, Stanford, CA, USA

STANFORD SCHOOL OF MEDICINE
Stanford University Medical Center

FAU FRIEDRICH-ALEXANDER UNIVERSITÄT ERLANGEN-NÜRNBERG
TECHNISCHE FAKULTÄT

I. Introduction

Fan-Beam Computed Tomography

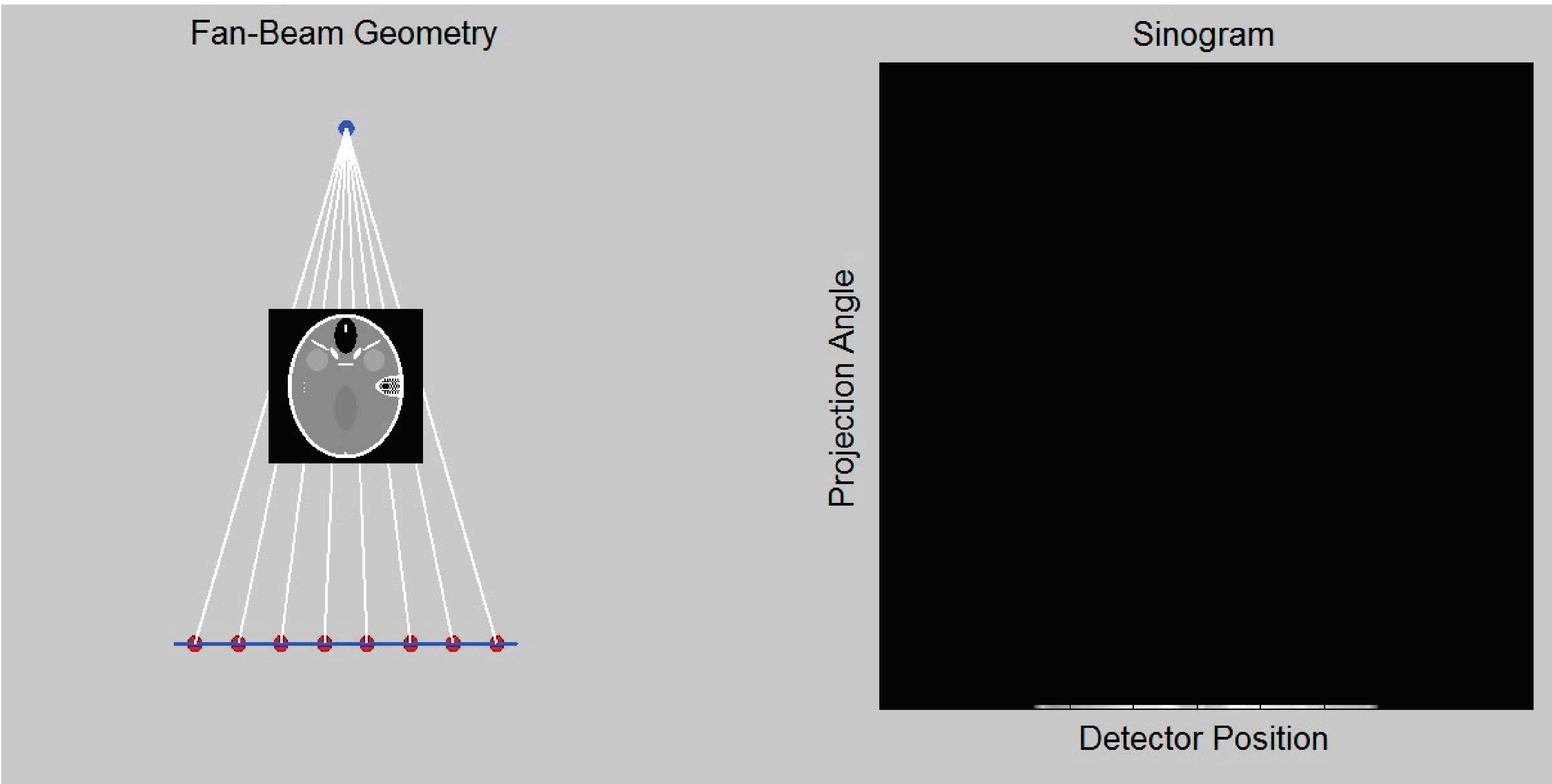

What happens when the patient is moving?

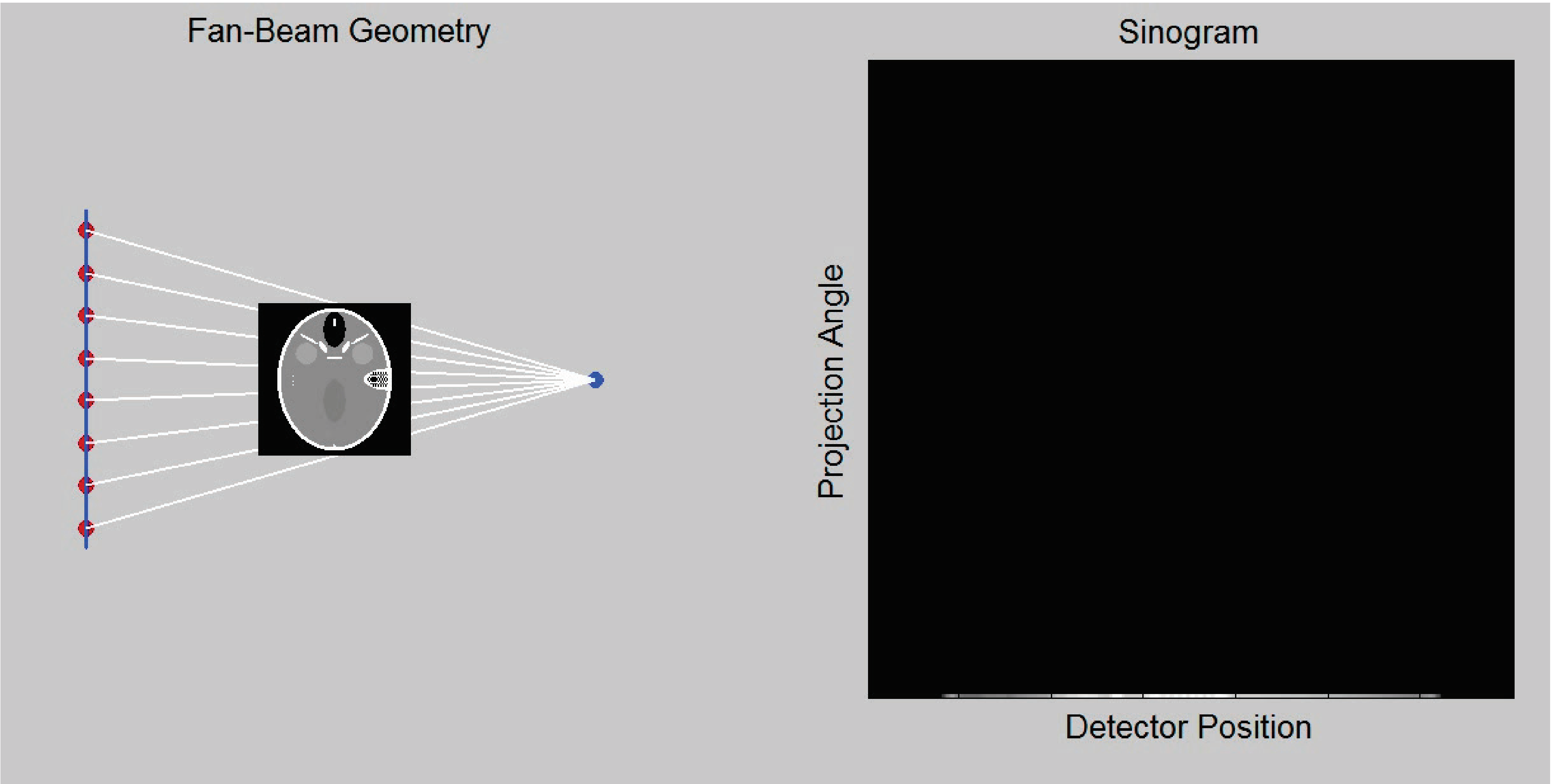

What happens when the patient is moving?

- Projections do not fit to each other
- High streaking artifacts
- Loss of structural information
- Overlapping streaks might cause low-frequency error

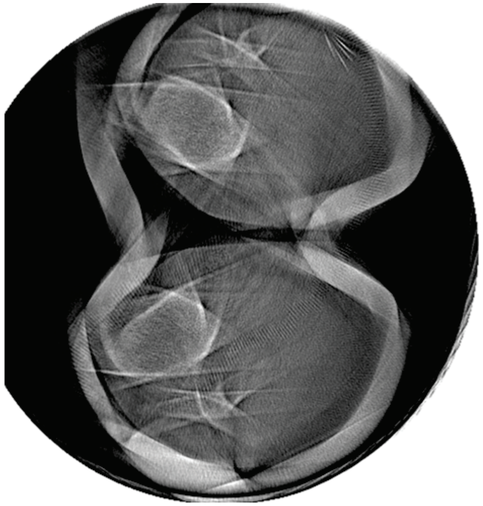

[Choi2014] Choi, J.-H., Maier, A., Keil, A., Pal, S., McWalter, E. J., Beaupré, G. S., … Fahrig, R. (2014). Fiducial marker-based correction for involuntary motion in weight-bearing C-arm CT scanning of knees. II. Experiment. Medical Physics, 41(6), 061902.

II. Fourier Properties of the Sinogram

Fourier Properties of the Sinogram – Parallel Beam

- Fourier transform of the sinogram contains triangular zero regions [Edholm1986]
- Regions depend on:
  - The extent of the object
  - The scanner geometry
- Spectrum axially symmetric
- Only valid for parallel beam geometry

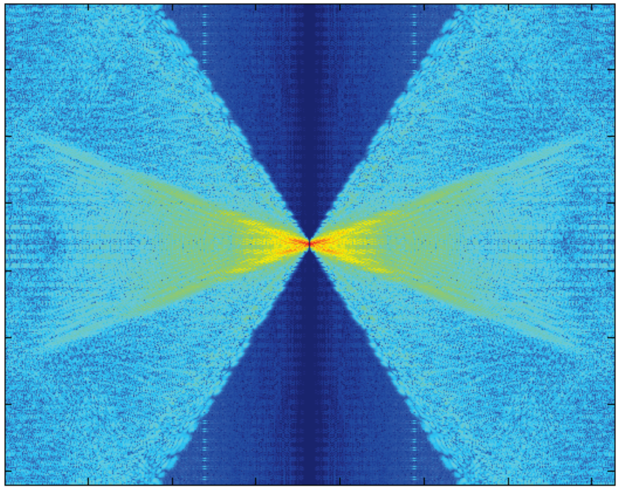

[Edholm1986] Edholm et. al., B. (1986). Novel Properties Of The Fourier Decomposition Of The Sinogram, *Proc. SPIE 0671, Physics and Engineering of Computerized Multidimensional Imaging and Processing* (pp. 8–18).

Fourier Properties of the Sinogram – Fan Beam

- Extension to fan-beam geometry [Mazin2010]
- Not fully analytically derived
- No longer axially symmetric
- Triangle size still depends on object size and scanner geometry

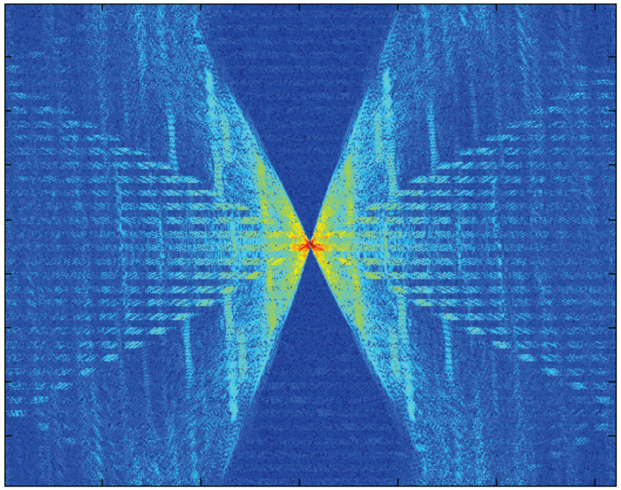

[Mazin2010] Mazin, S. R., & Pelc, N. J. (2010). Fourier properties of the fan-beam sinogram. Medical Physics, 37(4), 1674–1680.

Fourier Properties of the Sinogram – Fan Beam

- For flat detector fan-beam geometry the zero regions are given by:

$$\left| \frac{\omega}{\omega - \xi(L+D)} \right| > \frac{r_p}{L}$$

ω	Frequency variable for projection angle
ξ	Frequency variable for detector position
L	Source-to-patient distance
D	Detector-to-patient distance
r_p	Maximum radius of the object

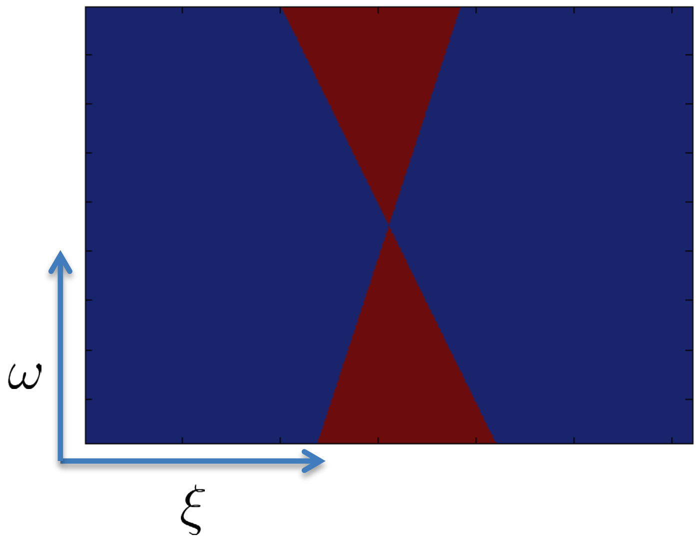

[Mazin2010] Mazin, S. R., & Pelc, N. J. (2010). Fourier properties of the fan-beam sinogram. Medical Physics, 37(4), 1674–1680.

What happens when the patient is moving?

No Motion:
$\text{MSE} = 1.22 \times 10^3$

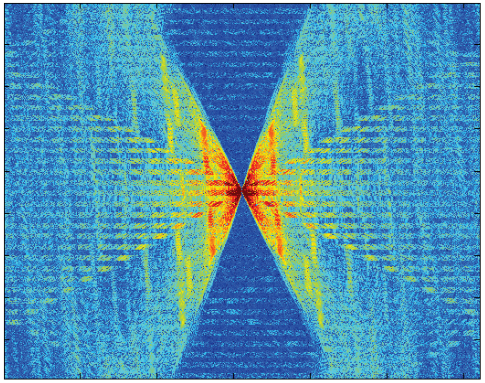

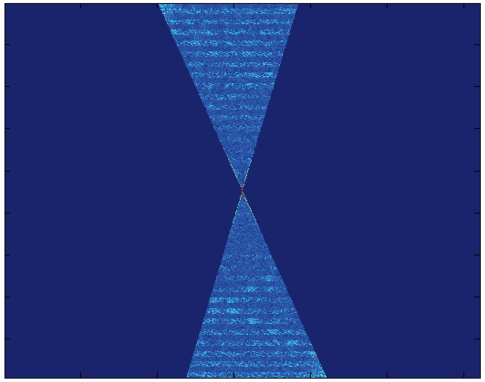

With Motion:
$\text{MSE} = 2.42 \times 10^5$

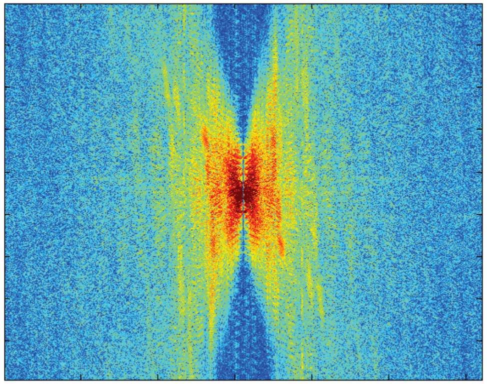

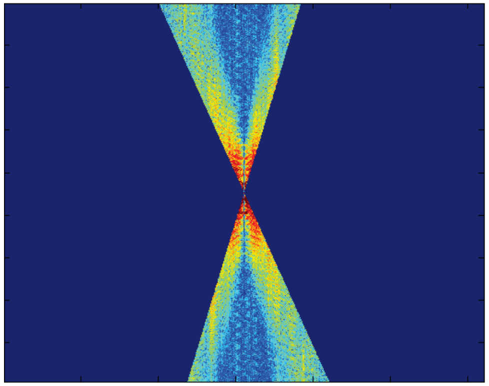

III. Methods

Detector-Based Sinogram Correction

- Translational motion can be approximated by a shift of projections
- Align projections such that they optimize a certain quality measure
- Can we use the fourier-constraint as a quality measure?

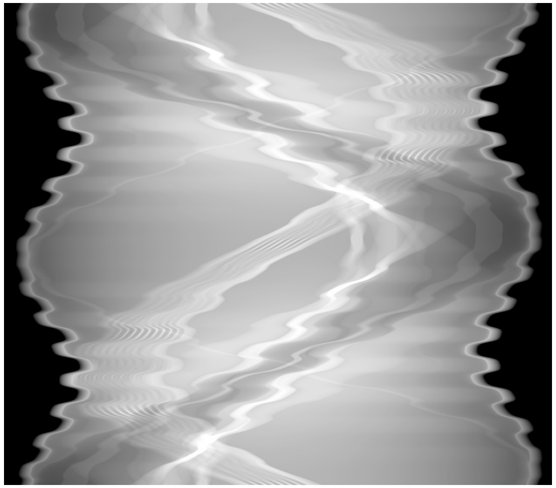

- Idea: Use energy in triangular spectral regions as error function

$$e(\mathbf{P}) = \left\| \mathbf{F}_\xi \, \mathbf{P} \, \mathbf{F}_\omega \circ \mathbf{W} \right\|_\mathrm{F}^2$$

Detector-Based Sinogram Correction

- Incorporate shifts into error function

$$\mathbf{t} = \arg\min_{\hat{\mathbf{t}}} \left\| \mathbf{F}_\xi \, \mathbf{P}_{\hat{\mathbf{t}}} \, \mathbf{F}_\omega \circ \mathbf{W} \right\|_{\mathrm{F}}^2$$

- Shift can be expressed in Fourier domain:

$$[t_1, \cdots, t_N] = \arg\min_{[t_1, \cdots, t_N]} \left\| \left(\left(\mathbf{F}_\xi \, \mathbf{P} \right) \mathbf{T} \right) \, \mathbf{F}_\omega \circ \mathbf{W} \right\|_{\mathrm{F}}^2$$

$$\mathbf{T} = \begin{pmatrix} e^{-i\frac{2\pi\xi}{M}t_1} & 0 & \cdots & 0 \\ 0 & e^{-i\frac{2\pi\xi}{M}t_2} & \cdots & 0 \\ \vdots & \vdots & \ddots & \vdots \\ 0 & 0 & \cdots & e^{-i\frac{2\pi\xi}{M}t_N} \end{pmatrix}$$

IV. Evaluation and Results

Evaluation Setup

- Phantom study using the central slice of the FORBILD head phantom

Parameter	Symbol/Unit	High-quality	Low-quality
Source-patient-distance	L	600	600
Detector-patient-distance	D	0	0
Approx. object extent [mm]	r_p	122.5	122.5
#Detector cells	M	1240	620
Detector spacing [mm]	du	0.25	0.5
#Projections	N	892	240
Angular spacing [degree]	$d\beta$	0.404	1.5
Reconstruction size	$R_x \times R_y$	2048×2048	2048×2048
Pixel size	[mm×mm]	0.125×0.125	0.125×0.125

Evaluation Setup

- Accelerated, periodic translation as simulated motion

$$t_x(\beta) = \hat{t}_x \left(\frac{2}{1 + \exp\left(a \cos\left(k\beta\right)\right)} - 1 \right)$$

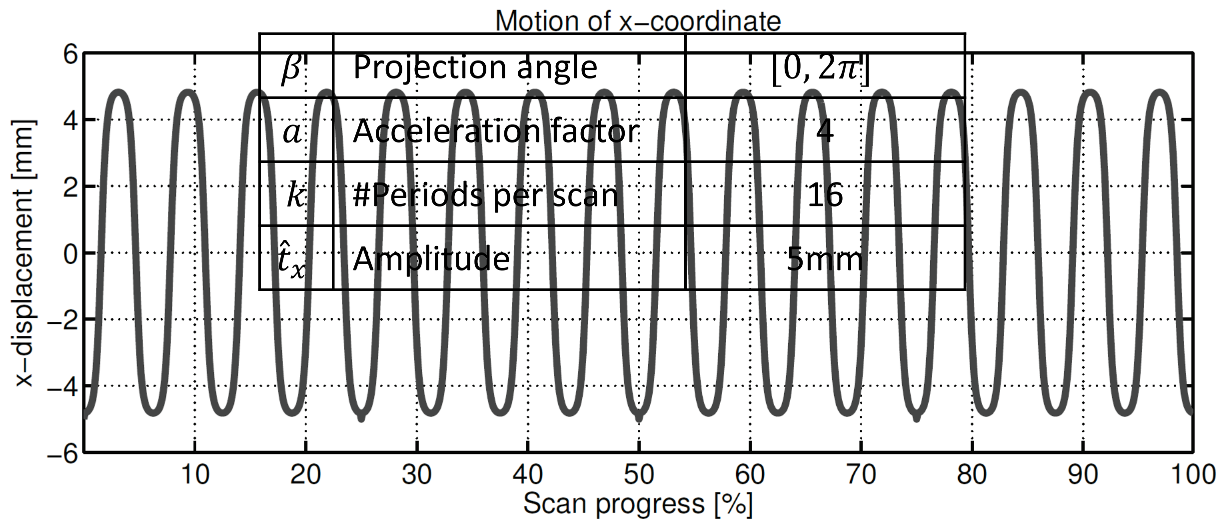

β	Projection angle	$[0, 2\pi]$
a	Acceleration factor	4
k	#Periods per scan	16
$\hat{t}_x$	Amplitude	5mm

Evaluation Setup

- Physical setup
  - High-quality: Energy 80keV (monochromatic)
    Noise-free
  - Low-quality: Energy 55keV (monochromatic)
    30000 photons

- Numerical optimization:
  - Multi-resolution approach
  - Quasi-Newton L-BFGS algorithm (Matlab‘s „fminunc“)

- Motion compensated backprojection [Schäfer2006]

[Schäfer2006] Schäfer, D., Borgert, J., Rasche, V., & Grass, M. (2006). Motion-compensated and gated cone beam filtered back-projection for 3-D rotational X-ray angiography. Medical Imaging, IEEE Transactions on, 25(7), 898–906.

Qualitative Results – High-Quality

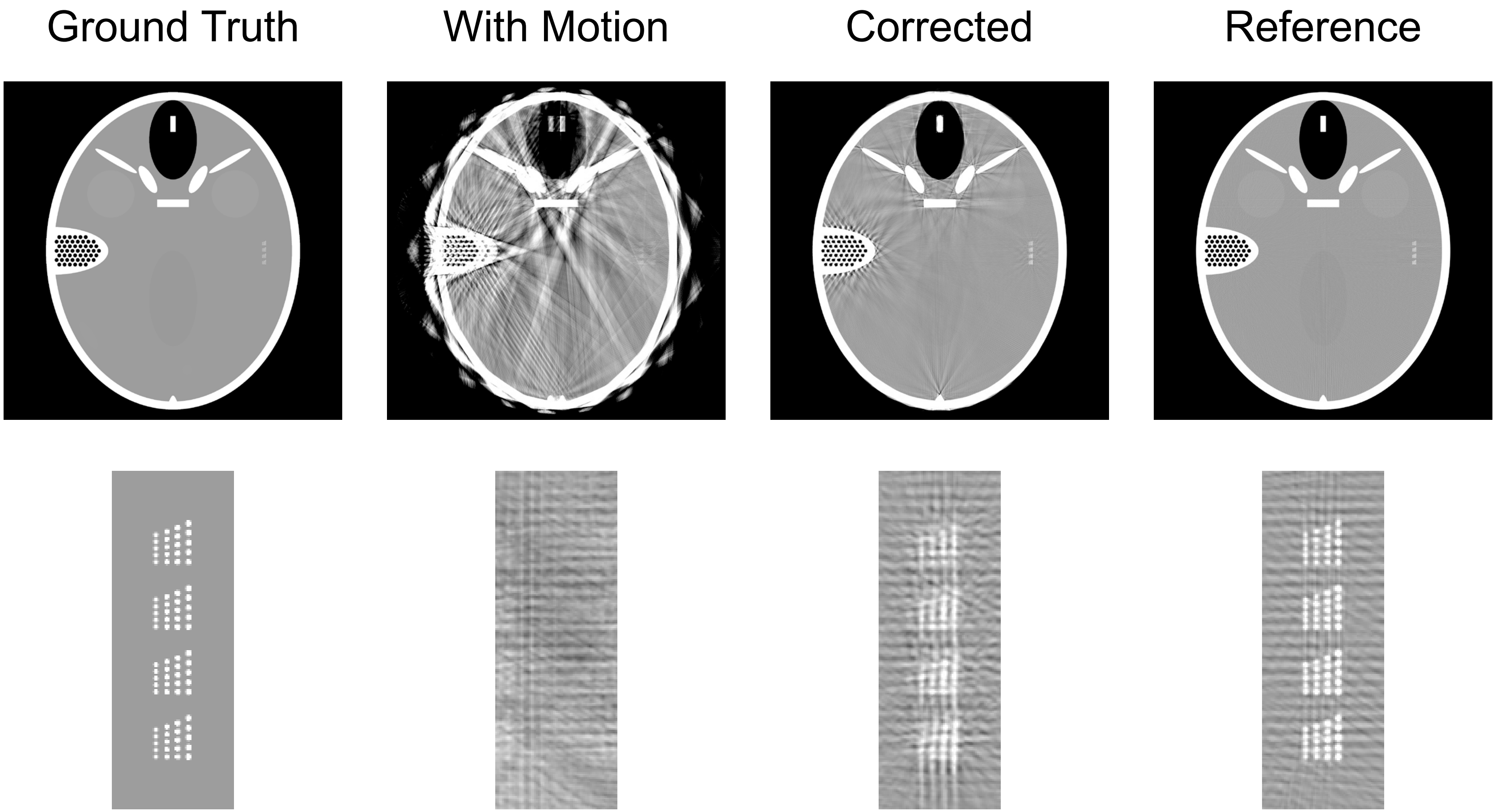

Qualitative Results – Low-Quality

Ground Truth | With Motion | Corrected | Reference

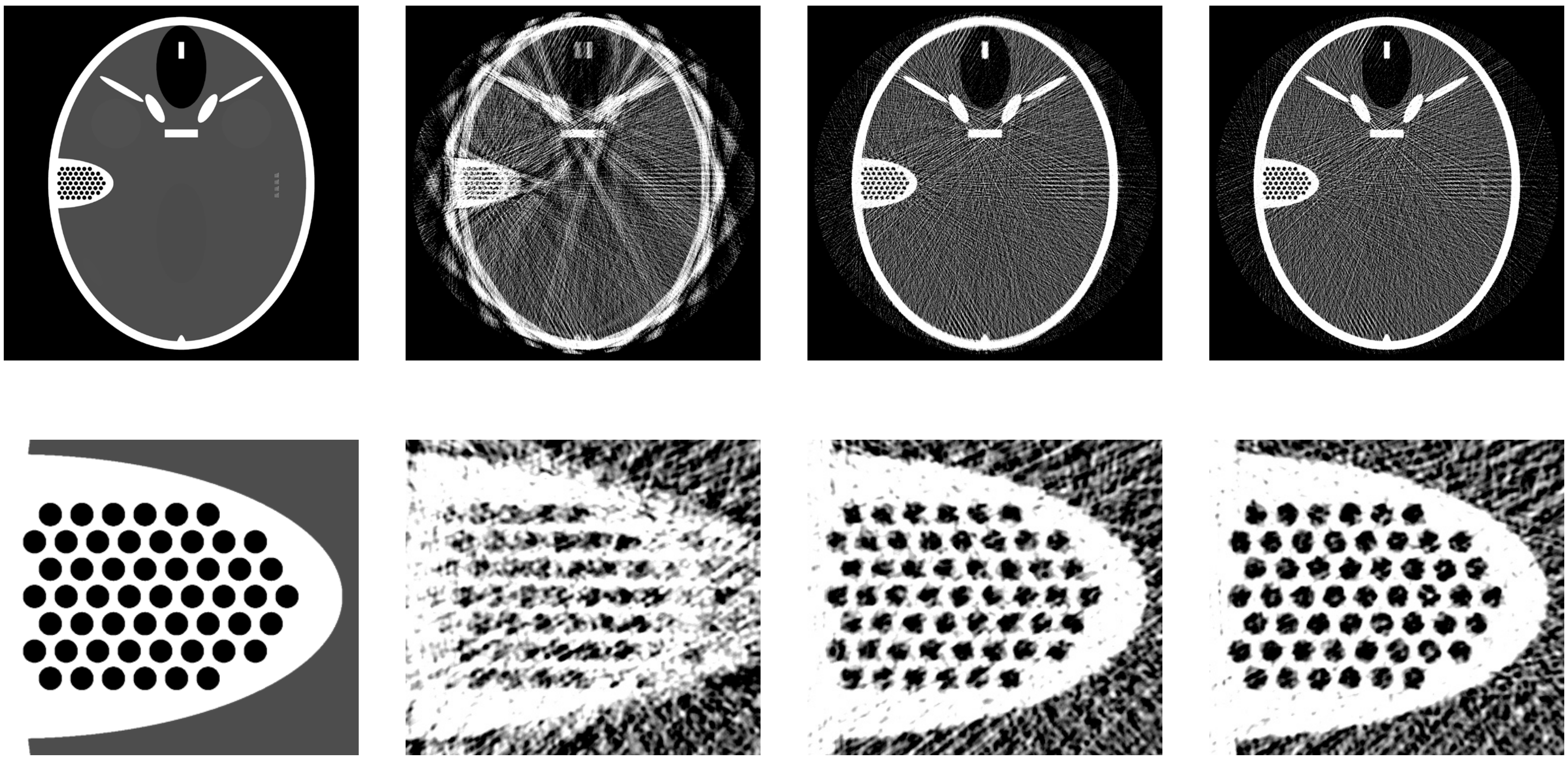

Qualitative Results – Sinogram/Spectra

With Motion | Corrected | Reference

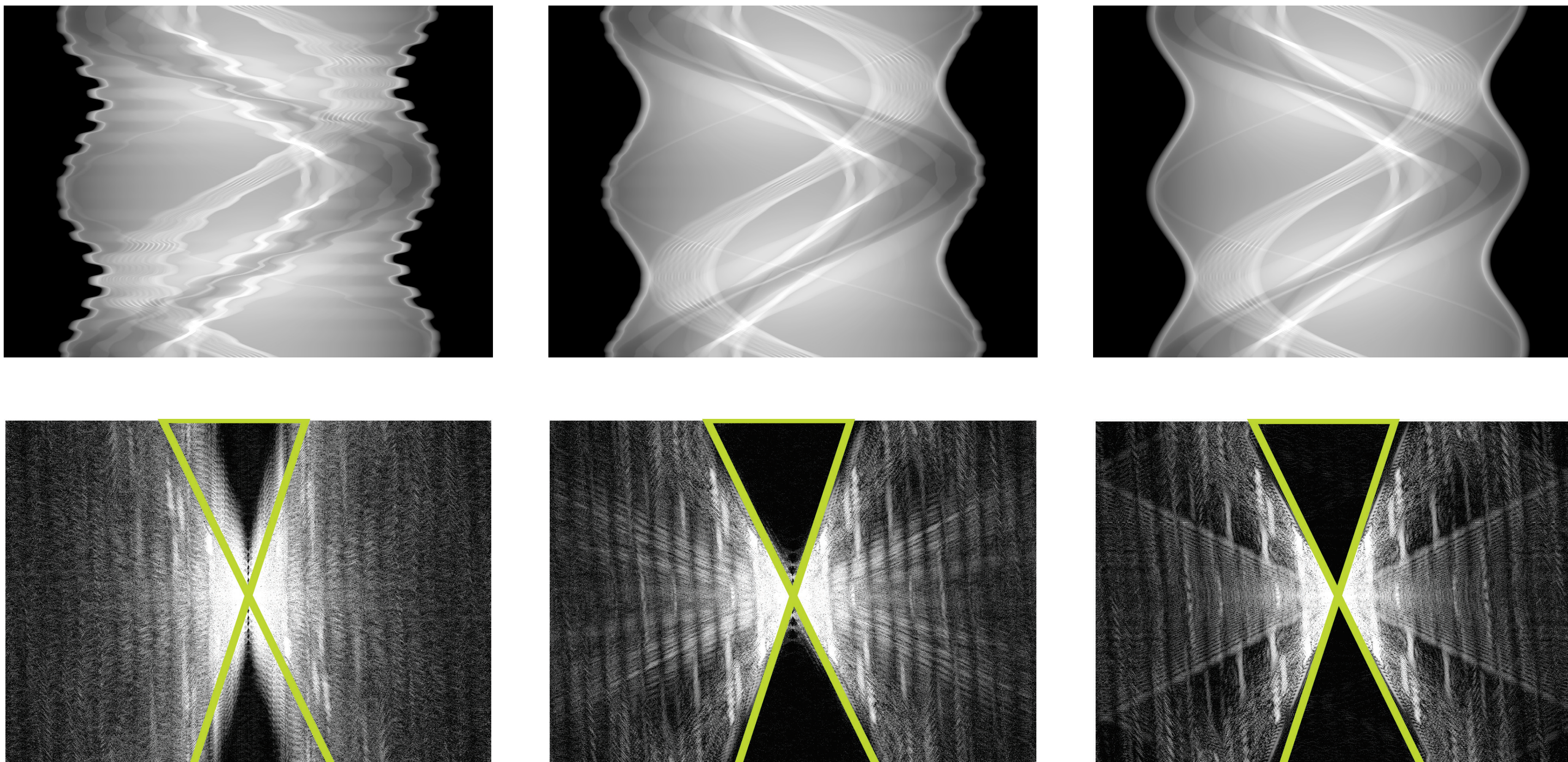

Quantitative Results – Error Function + rRMSE

	Measure	With motion	Corrected	Reference
High-quality	rRMSE [%]	20.35	7.09	2.48
	$e(\mathbf{P})$ [$\times 10^6$]	1648.49	32.35	0.34
Low-quality	rRMSE [%]	25.12	13.97	12.57
	$e(\mathbf{P})$ [$\times 10^6$]	109.55	6.32	4.12

V. Recent – Preliminary Results

Results With Additional Scaling

With Motion | Shifts Only | Shifts + Scaling | Reference

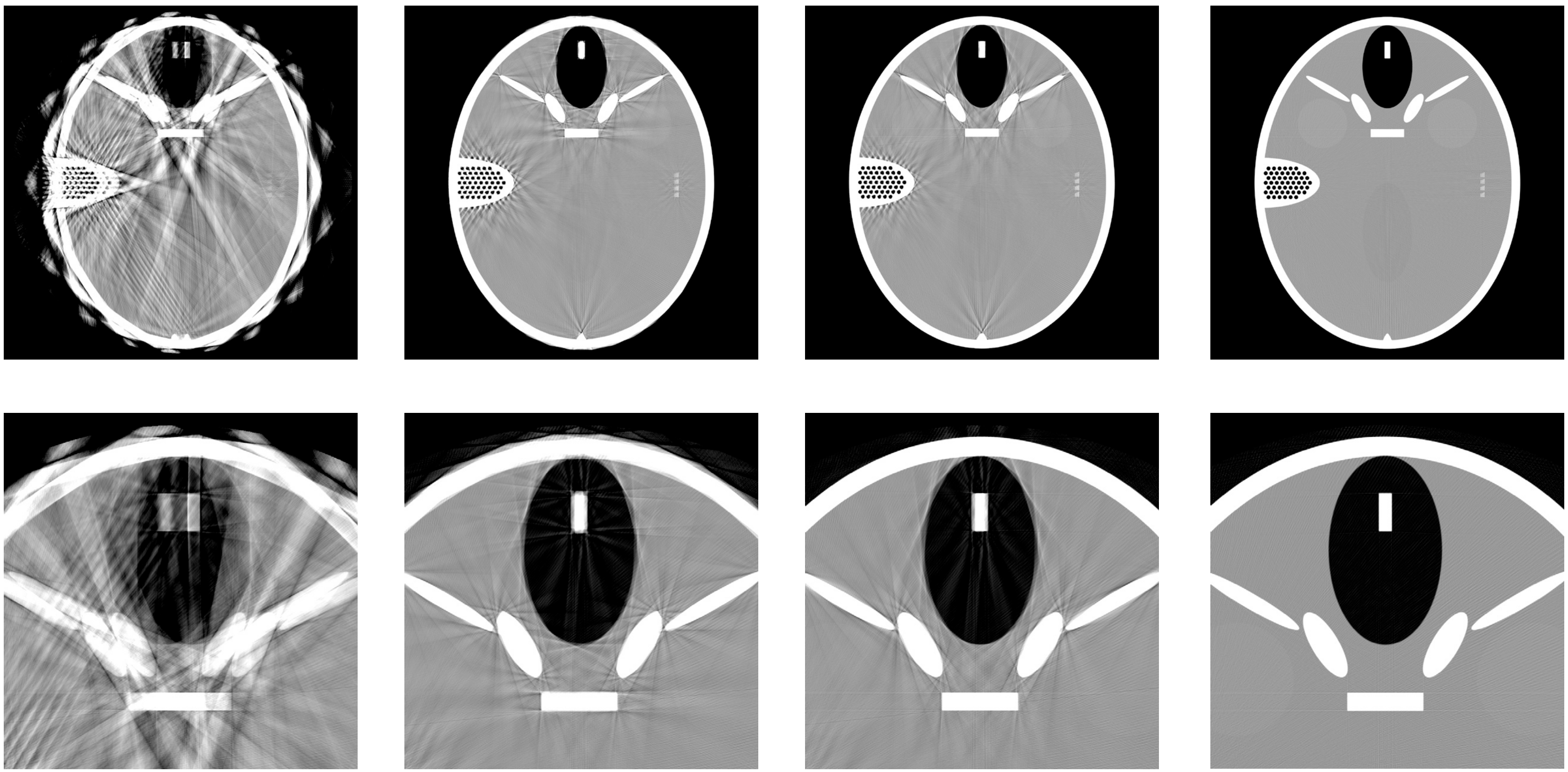

Results With Additional Scaling

With Motion | Shifts Only | Shifts + Scaling | Reference

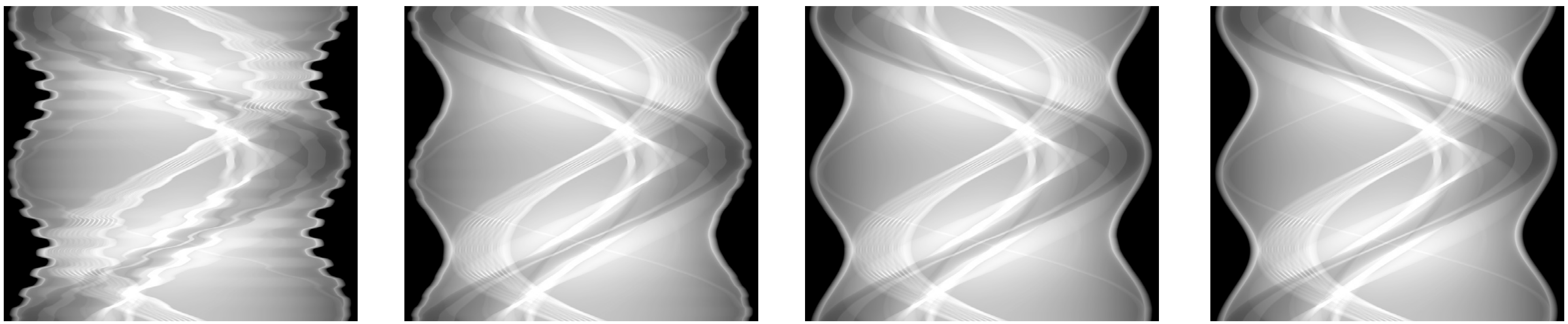

rRMSE [%]	With motion	Shifts Only	Shifts + Scaling	Reference
High-quality	20.35	7.09	4.47	2.48
Low-quality	25.12	13.97	13.77	12.57

VI. Conclusion / Outlook

Conclusion

- Zero regions of the sinogram's spectrum can be used as error function
- Efficient implementation by using the shift theorem
- Substantial increase of image quality compared to no correction
- Motion parallel to detector is sufficiently compensated by shifts
- Motion orthogonal to the detector can be corrected by scaling
- Still some residual streaking around fine structures

Challenges / Future work

- Full scan (360°) is required
  - Short scan can be extended to full-scan (Interpolation)
- Truncation will influence the zero condition
  - We are currently working on a truncation correction
- Object needs to be centered
- How about cone-beam geometry

Thanks for your attention! Questions?

STANFORD
SCHOOL OF MEDICINE
Stanford University Medical Center

FRIEDRICH-ALEXANDER
UNIVERSITÄT
ERLANGEN-NÜRNBERG
TECHNISCHE FAKULTÄT

Detector-Based Sinogram Correction

- Partial derivative w.r.t. detector shifts

$$
\begin{aligned}
\frac{\partial}{\partial t_n} e(\mathbf{P}_{\hat{\mathbf{t}}}) &= \frac{\partial}{\partial t_n} \left\| \left(\left(\mathbf{F}_\xi \, \mathbf{P} \right) \mathbf{T} \right) \mathbf{F}_\omega \circ \mathbf{W} \right\|_\mathrm{F}^2 \\
&= \frac{\partial}{\partial t_n} \left\| \mathbf{X} \right\|_\mathrm{F}^2 \\
&= \frac{\partial}{\partial t_n} \mathrm{Tr} \left(\mathbf{X} \mathbf{X}^\mathrm{H} \right) \\
&= \mathrm{Tr} \left(\left(\frac{\partial}{\partial t_n} \mathbf{X} \right) \mathbf{X}^\mathrm{H} + \mathbf{X} \left(\frac{\partial}{\partial t_n} \mathbf{X} \right)^\mathrm{H} \right)
\end{aligned}
$$

Detector-Based Sinogram Correction

- Partial derivative w.r.t. detector shifts

$$
\begin{aligned}
\frac{\partial}{\partial t_n}\mathbf{X} &= \frac{\partial}{\partial t_n}\Big(((\mathbf{F}_\xi\,\mathbf{P})\,\mathbf{T})\,\mathbf{F}_\omega \circ \mathbf{W}\Big) \\
&= \left((\mathbf{F}_\xi\,\mathbf{P}) \frac{\partial}{\partial t_n}\mathbf{T}\right) \mathbf{F}_\omega \circ \mathbf{W} \\
&= \left((\mathbf{F}_\xi\,\mathbf{P})(-i\frac{2\pi\xi}{M}\exp(-i\frac{2\pi\xi}{M}t_n)\mathbf{J}^{nn})\right) \mathbf{F}_\omega \circ \mathbf{W}
\end{aligned}
$$

Evaluation Setup

- Accelerated, periodic translation as simulated motion

$$t_x(\beta) = \hat{t}_x \left(\frac{2}{1 + \exp\left(a \cos\left(k\beta\right)\right)} - 1 \right)$$

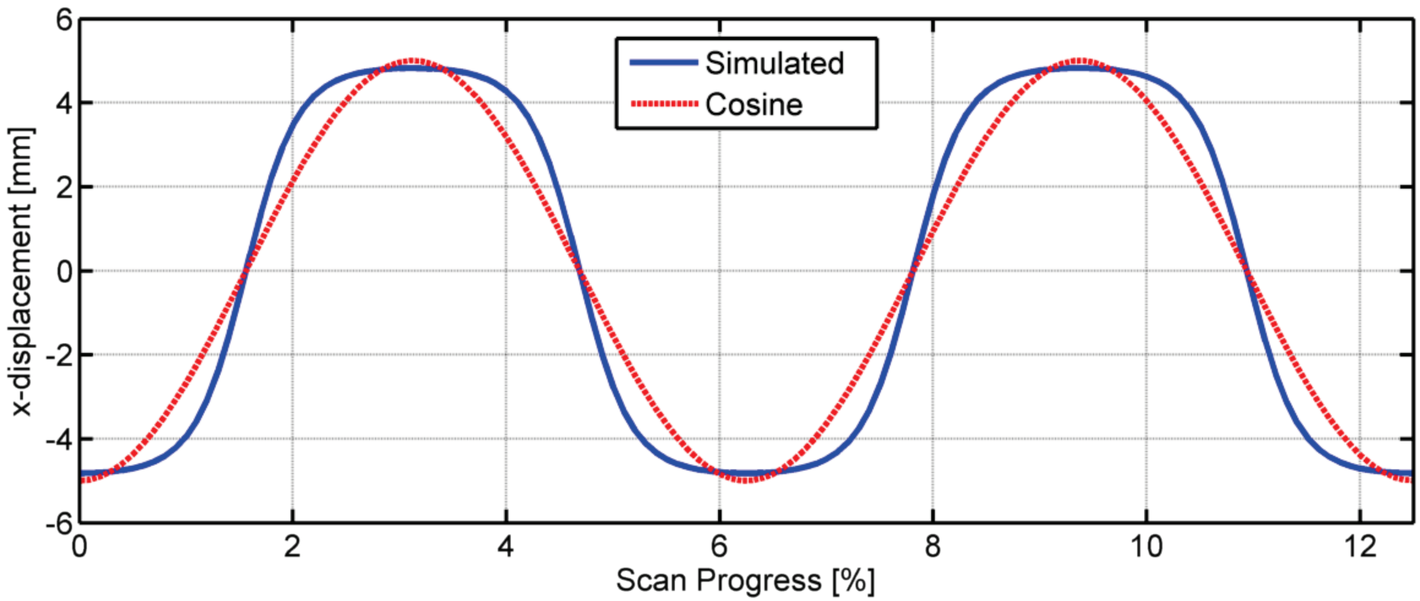

Quantitative Results – Estimated Motion On Detector

- High-quality:

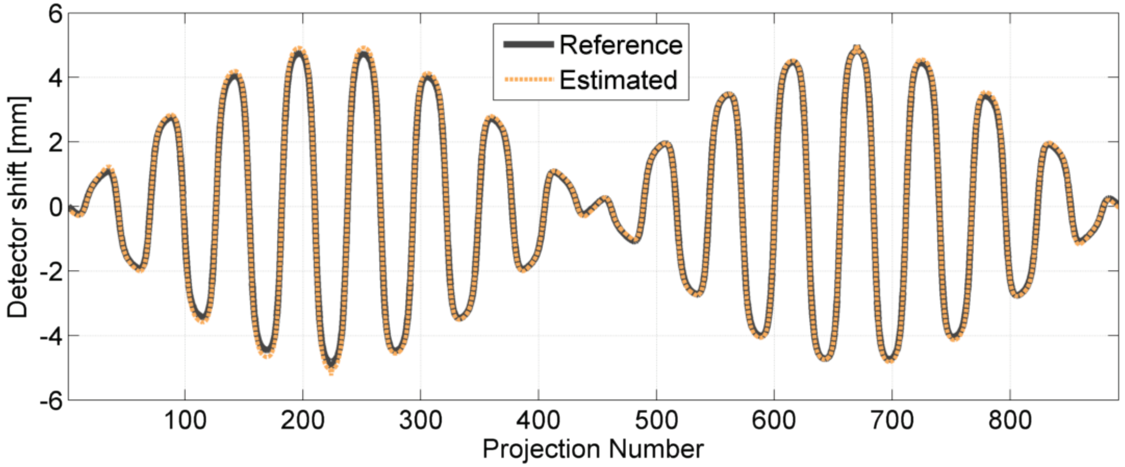

- Low-quality:

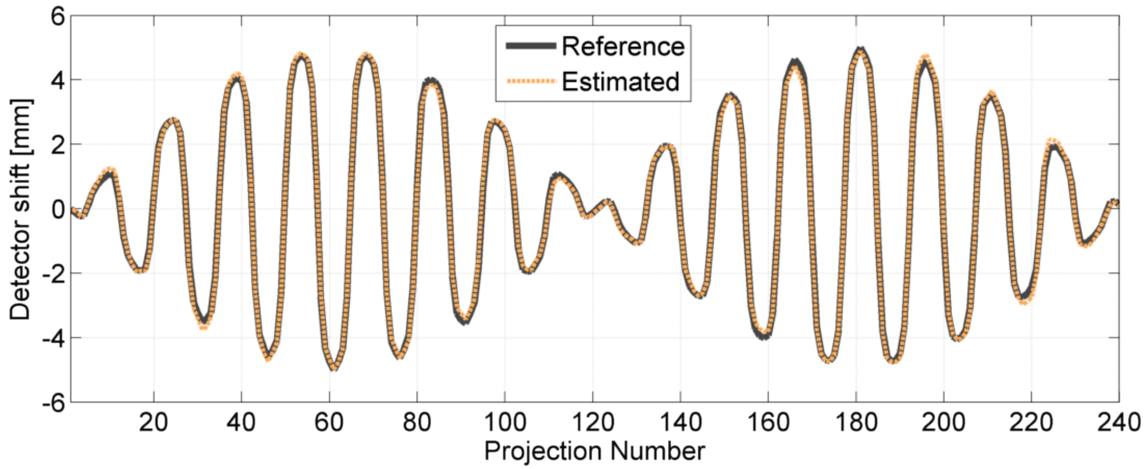

References

Consistency Properties

- Edholm et. al., (1986). Novel Properties Of The Fourier Decomposition Of The Sinogram, Proc. SPIE 0671, Physics and Engineering of Computerized Multidimensional Imaging and Processing (pp. 8–18).
- Mazin, S. R., & Pelc, N. J. (2010). Fourier properties of the fan-beam sinogram. Medical Physics, 37(4), 1674–1680.
- Yu et. al., (2006). Data consistency based translational motion artifact reduction in fan-beam CT. *IEEE Transactions on Medical Imaging*, *25*(6), 792–803.
- Clackdoyle, R., & Desbat, L. (2013). Full data consistency conditions for cone-beam projections with sources on a plane. *Physics in Medicine and Biology*, *58*(23), 8437.

Reconstruction and Motion Compensation

- Schäfer, D., Borgert, J., Rasche, V., & Grass, M. (2006). Motion-compensated and gated cone beam filtered back-projection for 3-D rotational X-ray angiography. Medical Imaging, IEEE Transactions on, 25(7), 898–906.
- Schwemmer, C., Rohkohl, C., Lauritsch, G., Müller, K., & Hornegger, J. (2013). Residual motion compensation in ECG-gated interventional cardiac vasculature reconstruction. *Physics in Medicine and Biology*, *58*(11), 3717.
- Choi, J.-H., Maier, A., Keil, A., Pal, S., McWalter, E. J., Beaupré, G. S., … Fahrig, R. (2014). Fiducial marker-based correction for involuntary motion in weight-bearing C-arm CT scanning of knees. II. Experiment. Medical Physics, 41(6), 061902.